INT. J. NUM. METH. HEAT FLUID FLOW, VOL. 3, 133–143 (1993)

NATURAL CONVECTION IN PARTITIONED ENCLOSURES WITH LOCALIZED HEATING

E. NTIBARUFATA, M. HASNAOUI, E. BILGEN AND P. VASSEUR

Departement de Mécanique, Ecole Polytechnique, CP 6079, St A, Montréal, PQ, H3C 3A7, Canada

ABSTRACT

The aim of the present investigation was to study numerically the natural convection in partitioned enclosures with localized heating from below. Two-dimensional equations of conservation of mass, momentum and energy, with the Boussinesq approximation are solved using finite difference method. Various geometrical parameters were: aspect ratio $A = 0.4–0.6$, isothermal surface length $B = 0.5$, its position $C = 0.3$, partition position $D = 0.5–1.0$, its length $E = 0.2–0.6$, heat source length $X = 0.05–1.00$, and its position ε = variable. The Rayleigh number was varied from 10^3 to 10^6. The results are reduced in terms of the normalized Nusselt number as a function of the Rayleigh number, and other non-dimensional geometrical parameters. The isotherms and streamlines are produced for various Rayleigh numbers and geometrical conditions.

KEY WORDS Natural convection Finite difference discretization

NOMENCLATURE

A aspect ratio, H'/L'
B dimensionless length of isothermal surface, h'/H'
C dimensionless position of isothermal surface, h_1'/H'
D dimensionless position of the partition, L''/L'
E dimensionless partition length, h_1''/H'
h' length of the isothermal surface (m)
h_1' position of the isothermal surface (m)
h_1'' partition length (m)
H' cavity height (m)
k thermal conductivity of fluid (W/m·K)
L_1' position of the heated element (m)
L_2' length of the heated element (m)
L' cavity width (m)
L'' position of partition (m)
Nu normalized mean Nusselt number, (8)
Pr Prandtl number, ν/α
q' constant heat flux (W/m^2)
Ra Rayleigh number, $(g\beta q' H'^4)/(k\nu\alpha)$
t dimensionless time, $t'\alpha/H'^2$
T dimensionless temperature, $(T' - T_C')/(q'H'/k)$
u, v dimensionless velocities in x and y directions, $(u', v')H'/\alpha$
x, y dimensionless Cartesian coordinates, $(x', y')/H'$
X dimensionless length of the heated element, L_2'/L'

Greek

α thermal diffusivity of fluid (m^2/sec)
β volumetric coefficient of thermal expansion (K^{-1})
ε dimensionless position of the heated element, $(L_1' + L_2'/2)/H'$
Ω dimensionless vorticity, $\Omega' H'^2/\alpha$
ν kinematic viscosity (m^2/sec)

0961–5539/93/020133–11$2.00

Received June 1992

ρ	fluid density (kg/m^3)	loc	local
Ψ	dimensionless stream function, Ψ'/α	W	heated wall

Subscript

C cold wall

Superscript

dimensional variables

INTRODUCTION

In direct gain passive systems, the solar radiation transmitted through the window strikes the internal surfaces of the dwelling. In steady state conditions, the dwelling air being quasi-transparent to incoming radiation, the radiation is absorbed by the internal surfaces, which is in turn transferred in part by infra-red radiation and in major part by natural convection to the dwelling air. The energy gained is lost, in major part, through quasi-isothermal windows, which are in contact with outside air at constant temperature. The dwelling internal and external surfaces are usually well insulated, therefore they are quasi-adiabatic. In general, the dwelling may be made of two adjacent rooms connected with a passage way. Both rooms may have windows opposite to each other. The solar radiation through a window is received and absorbed by the bottom surface. Therefore, the length and position of the heated surface depend on the sun's position, window's geometry and its orientation. The absorbed heat is usually transferred to the air by a constant heat flux. The overall system thermal performance is determined by various parameters, such as window size, its orientation, thermal resistance, thermal characteristics of the internal surfaces and position of the sun. The problem can be simplified by considering the dwelling as a two-dimensional enclosure with one passage way and two opposite windows. Further, heat transfer by infra-red radiation and conduction with respect to natural convection may be neglected. With these assumptions, the problem becomes one of natural convection heat transfer in two-dimensional partitioned enclosures with localized heating from below.

A literature review shows that most of the previous work has addressed natural convection in enclosures due to either a vertically or horizontally imposed temperature difference. However, little work has been carried out on flows driven by localized heating from below, one side or both. Torrance and Rockett[1] numerically studied the convection of air, in a vertical cylindrical enclosure, induced by a small hot spot centrally located on the bottom. The theoretical flows were in good agreement with the experimental results[2]. Tamotsu *et al.*[3] experimentally and numerically investigated natural convection in a rectangular enclosed cavity, of which a part of the bottom was heated and the other walls were kept at a low constant temperature. The influence of the Rayleigh number, up to $Ra = 6.9 \times 10^5$, was discussed. The natural convection in an inclined box with the lower half surface heated and the other half insulated was investigated experimentally and numerically by Chao *et al.*[4]. It was found that the asymmetry due to insulating half of the heated surface resulted in circulations for all positive Rayleigh numbers. An experimental investigation was conducted by Kamotani *et al.*[5] to study natural convection heat transfer in a water layer with localized heating from below. The problem of multiplicity of solution and heat transfer in rectangular cavities partially heated from below was also studied earlier by Hasnaoui *et al.*[6]. In this problem, the upper surface was cooled at a constant temperature and a portion of the bottom surface was isothermally heated while the rest of it and the vertical walls were adiabatic.

The aim of the present study was to study numerically the natural convection in two-dimensional partitioned enclosures with localized heating from below. Part of the two vertical surfaces representing windows is assumed to be isothermal, the rest adiabatic.

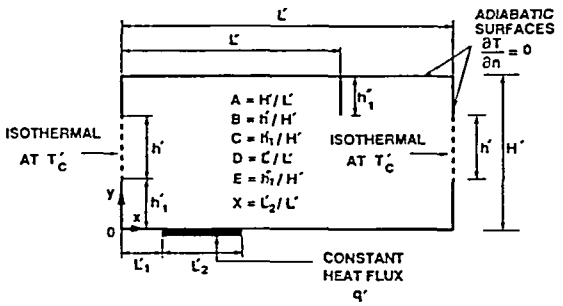

Figure 1 · Geometry and boundary conditions of the problem

PROBLEM FORMULATION

The study domain is a two-dimensional rectangular enclosure of dimensions $L' \times H'$ with a partial partition as shown in *Figure 1*. A portion of the bottom releases energy with a constant flux q'. The other portions are adiabatic, except part of the vertical surfaces, which is maintained at a constant temperature T'_C. The heated element is identified by its position $(\varepsilon = (L'_1 + L'_2/2)/H')$ and its length $(X = L'_2/L')$. If the flow and heat transfer are two-dimensional and the Boussinesq approximation holds, the dimensionless governing equations are written as:

$$\frac{\partial \Omega}{\partial t} + \frac{\partial u\Omega}{\partial x} + \frac{\partial v\Omega}{\partial y} = -RaPr\frac{\partial T}{\partial x} + Pr\nabla^2\Omega \tag{1}$$

$$\nabla^2\Psi = -\Omega \tag{2}$$

$$\frac{\partial T}{\partial t} + \frac{\partial uT}{\partial x} + \frac{\partial vT}{\partial y} = \nabla^2 T \tag{3}$$

where

$$u = -\frac{\partial \Psi}{\partial y} \qquad v = \frac{\partial \Psi}{\partial x} \tag{4}$$

$$\Omega = \frac{\partial u}{\partial y} - \frac{\partial v}{\partial x} \tag{5}$$

Equations (1) to (5) have been reduced to dimensionless form by introducing the scales defined in the Nomenclature.

No slip boundary conditions are considered for velocity components along the walls. The vorticity boundary values were calculated from the second order approximation of Woods[7]. For the temperature, the following conditions are used:

$$\left.\begin{aligned} &\frac{\partial T}{\partial y} = -1 && \text{for heated portion} \\ &T = 0 && \text{for isothermal surfaces} \\ &\frac{\partial T}{\partial n} = 0 && \text{for adiabatic portions} \end{aligned}\right\} \tag{6}$$

where the direction of n is the normal to the surface element considered.

The governing equations, with boundary conditions, complete the formulation of the problem. The controlling parameters are Ra, Pr, A, B, C, D, E, ε and X (see *Figure 1*).

The local heat transfer on the heating element, which is submitted to a constant heat flux q', is calculated as:

$$Nu_{\text{loc}} = \frac{q'H'}{(T'_W - T'_C)k} = \frac{1}{T_W} \tag{7}$$

The isothermal surface temperature T'_C, is considered as reference temperature. The mean normalized Nusselt number on the heating element is calculated as:

$$Nu = \frac{Q}{Q_C} \tag{8}$$

where Q is given by:

$$Q = \frac{A}{X}\int_{\varepsilon - X/2A}^{\varepsilon + X/2A} \frac{1}{T_W}\,\mathrm{d}x \tag{9}$$

where Q_C is the mean dimensionless heat transfer by pure conduction on the heating element surface calculated with (9) for $Ra = 0$.

NUMERICAL METHOD

The conservation equations (1) to (3) describing the flow and temperature fields in this problem were solved numerically using a finite-difference discretization procedure. Central-difference formulae were used for all spatial derivative terms, in the vorticity, energy and Poisson equations. A modified alternate direction implicit procedure was adapted to obtain from (1) and (3) the vorticity and temperature profiles. The finite-difference forms of the vorticity and energy equations were written in conservative form for the convective terms to preserve the conservative property[8]. Values of the stream function at all grid points were obtained with (2) via a successive over-relaxation method. Suitable values for the relaxation parameters were between 1.78 and 1.92. The velocities at all grid points were determined with (4) using updated values of the stream function. For each time step, the convergence criterion was:

$$\frac{\sum_{i,j} |\Psi_{i,j}^{n+1} - \Psi_{i,j}^{n}|}{\sum_{i,j} |\Psi_{i,j}^{n+1}|} \leqslant 10^{-4} \tag{10}$$

For the present work, uniform mesh sizes were used for both x and y directions. The boundary condition on the partition was ensured by using three grid points within its thickness. To study the effect of the thickness on the result, four and five grid points were also tried which showed a negligible effect. The grid sizes of 41, 61, 81, 161 in x direction with 21 in y direction were tried for various cases. For example, with $Ra = 10^6$ the results from various grid sizes compared to those with 161 × 21 showed that the maximum deviations were 0.9% in energy conservation, 3.25% in heat transfer, 1.02% in normalized Nusselt number and 1.97% in $\Psi_{\max}$. In view of the possible singular behaviour at the mixed boundaries[9], variations of $\Psi_{\max}$ and Nu with time were examined in each case and proper convergence to a steady state solution was ensured. Thus, most of the computations were carried out with 61 or 41 × 21 grid size. To ensure the

precision in some of the studies, computations were also carried out using 81 or 161 × 21 grid size. These will be pointed out when appropriate. Various time step sizes were tried and 0.0002 was used for most of the simulations.

The accuracy of the numerical model was verified by comparing results from the present investigation with several results reported in the literature[10]. Maximum differences were within 4% of the results compiled and discussed by De Vahl Davis and Jones[11]. The numerical model was validated also with that by Hasnaoui *et al.*[6] who studied the problem of rectangular cavity partially heated from below; the agreement was excellent.

RESULTS AND DISCUSSION

Flow fields, temperature fields and heat transfer rates for ranges of Rayleigh numbers from 10^3 to 10^6 are examined. The size of the isothermal sink $B = 0.50$, and its position $C = 0.30$ were kept constant. The aspect ratio A was varied from 0.40 to 0.60. The position of partition D was varied from 0.50 to 1.00, the size of the heat sources X from 0.05 to 1.0, the position of the heat source ε from 0 to 1 and the partition size E from 0.20 to 0.60. All results are presented for $Pr = 0.72$. First the results with $A = 0.50$, $D = 0.5$ and $E = 0.20$ will be presented and then their influences will be discussed.

The streamlines and isotherms for $Ra = 10^6$, $D = 0.5$, $X = 0.25$ and for various positions of the localized heat source ε are shown in *Figures 2a–2c* and for various X in *Figures 2d* and *2e*. In these Figures, the heat source is shown with a thick line and the isothermal sink with a thin line; the negative values of the stream function show a counter-clockwise circulation in the enclosure.

Figures 2a–2c show the effect of heat source position. When the heat source is at the corner, a large clockwise circulating cell is formed, which is responsible for transporting energy to the left and right isothermal sinks. The small cell above the large cell near the left upper part circulates counter-clockwise. The isotherms show a steep gradient of temperature above the heat source within the large cell. As the position of the heat source shifts towards the centre, *Figure 2b* shows two cells formed above the heat source, one counter-clockwise rotating cell near the left isothermal sink and another elongated, clockwise rotating cell on the right. The strength of the circulation is slightly larger in the counter-clockwise rotating cell. The isotherms show steep temperature gradients near the heat source and the left heat sink, with more heat transfer to the left. For the heat source positioned at the centre in *Figure 2c*, two symmetric cells are formed above the heat source, one on the left rotating counter-clockwise and the other on the right clockwise. The isotherms show a symmetric case with identical temperature gradients and heat transfer to both sides. Streamlines and isotherms (not shown here) were identical for $\varepsilon = 1.50$ and 1.75, which corresponded to the positions symmetric with respect to the centre of the enclosure. The effect of the heat source size is shown in *Figures 2d, b* and *e* for $X = 0.15$, 0.25 and 0.50 respectively. Streamlines and isotherms show similar trends, the strength of counter-clockwise circulation increasing with X: $\Psi_{min} = -14.59$ for $X = 0.15$, -16.48 for $X = 0.25$ and -20.25 for $X = 0.50$.

For constant geometrical parameters of $A = 0.5$, $B = 0.5$, $C = 0.3$, the mean normalized Nusselt number on the heat source at various Rayleigh numbers for various X and ε is calculated and shown in *Figures 3 a* to *f*. At $Ra = 10^3$, the heat transfer is dominated by conduction for all X and ε. For small size of heat source, X and position, ε the heat transfer is still dominated by conduction at higher Rayleigh numbers. In *Figure 3a* for $X = 0.05$ and $\varepsilon = 0.05$, which is almost a point heat source at the corner, the conduction dominant regime is observed up to $Ra = 10^5$. For $\varepsilon = 0.50$ and 1.00, the heat transfer is by conduction up to about 10^4. Similar trend is observed in *Figure 3b* and *3c* for $\varepsilon = 0.15$ and 0.25. For increasing Rayleigh number and size of heat source, the contribution of natural convection increases. *Figures 3a* to *f* show that Nu is an increasing function of X and with the exception of *Figures 3a* and *3b* at high Ra,

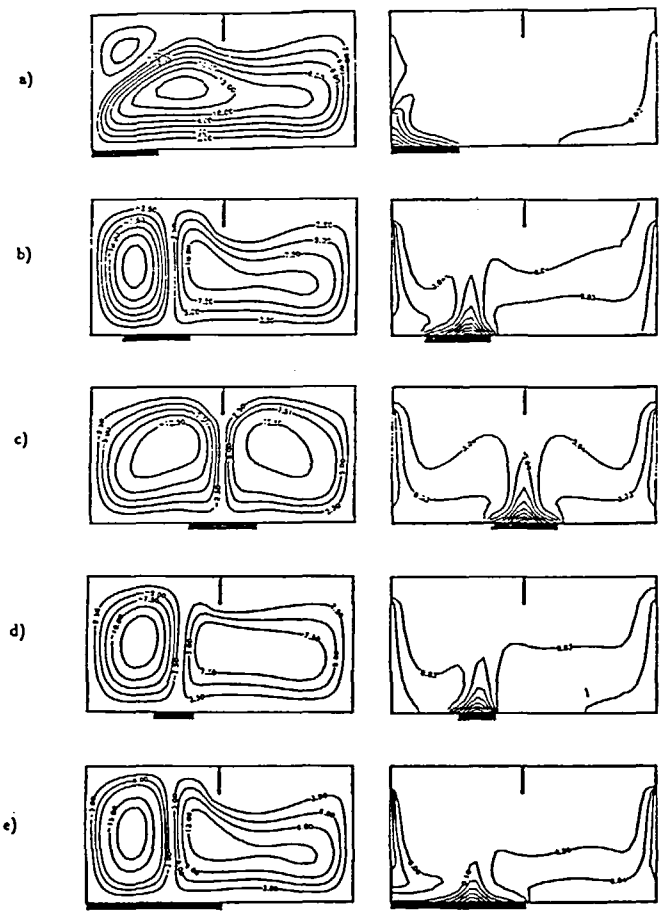

Figure 2 Steady-state streamlines (on the left) and isotherms (on the right) for $Ra = 10^6$, $A = 0.5$, $B = 0.5$, $C = 0.3$, $D = 0.5$: (a) $X = 0.25$, $\varepsilon = 0.25$, $\Psi_{max} = 15.09$, $\Psi_{min} = -4.88$; (b) $X = 0.25$, $\varepsilon = 0.5$, $\Psi_{max} = 12.08$, $\Psi_{min} = -16.48$; (c) $X = 0.25$, $\varepsilon = 1.0$, $\Psi_{max} = \pm 14.64$; (d) $X = 0.15$, $\varepsilon = 0.6$, $\Psi_{max} = 10.76$, $\Psi_{min} = -14.59$; (e) $X = 0.50$, $\varepsilon = 0.50$, $\Psi_{max} = 14.57$, $\Psi_{min} = -20.25$

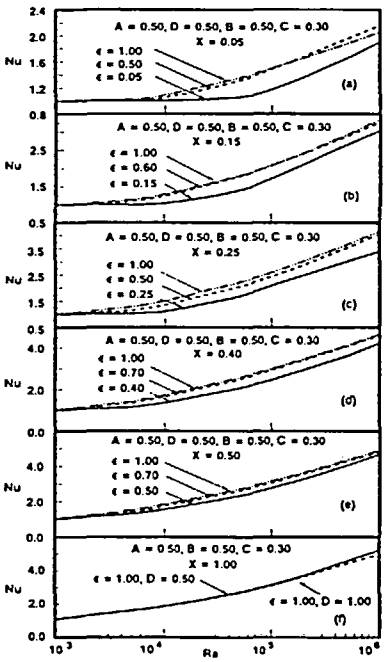

Figure 3 Normalized mean Nusselt number as a function of the Rayleigh number for $D = 0.50$, and various X and ε. (a) $X = 0.05$, (b) $X = 0.15$, (c) $X = 0.25$, (d) $X = 0.40$, (e) $X = 0.50$, (f) $X = 1.0$

an increasing function of ε. This is to be expected as the heat released will increase proportionately with the size of heat source. Also, as it was observed earlier with *Figure 2*, the convection increases for heat source positioned more centrally. The reason for the lower heat transfer in *Figures 3a* and *3b* when ε increases from 0.50 to 0.60 to 1.00 at high Ra is explained by examining the streamlines at $Ra = 10^6$. It was seen (not shown here) that the strength of circulation decreased in both cases with increasing ε. As discussed with *Figure 2*, the cases with $\varepsilon = 1.00$ resulted in identical heat transfer for a given X and Ra due to the symmetry of the problem.

Similar results are produced for $D = 0.75$ with the other constant parameters being the same. Streamlines and isotherms for the case of $X = 0.5$ and $Ra = 10^6$ for various ε are shown in *Figure 4*. *Figure 4a* shows that for the case of heat source attached to the left corner two cells are formed above the heat source, one counter-clockwise on the left and the other clockwise rotating and elongated on the right. Their strengths of circulation are $\Psi_{min} = -20.29$ and $\Psi_{max} = 15.55$ respectively. *Figure 4a* shows that the partition acts like a barrier and heat transfer is stronger to the left. The isotherms show steep gradients above the heat source and on the left

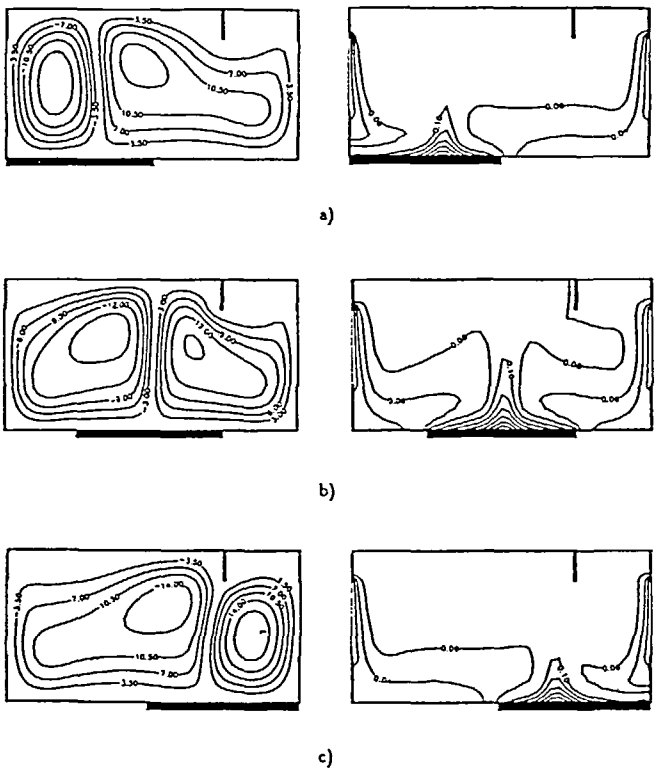

Figure 4 Steady-state streamlines (on the left) and isotherms (on the right) for $Ra = 10^6$, $A = 0.5$, $B = 0.5$, $C = 0.3$, $D = 0.75$ and $X = 0.50$. (a) $\varepsilon = 0.5$, $\Psi_{max} = 15.55$, $\Psi_{min} = -20.29$; (b) $\varepsilon = 1.0$, $\Psi_{max} = 15.49$, $\Psi_{min} = -16.93$; (c) $\varepsilon = 1.5$, $\Psi_{max} = 20.14$, $\Psi_{min} = -16.08$

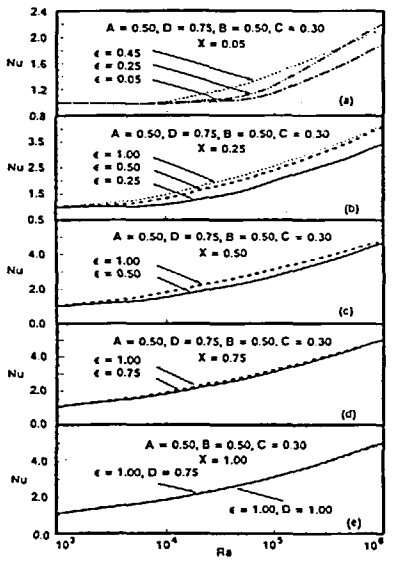

Figure 5 Normalized mean Nusselt number as a function of Rayleigh number for $D = 0.75$, and various X and ε. (a) $X = 0.05$, (b) $X = 0.25$, (c) $X = 0.5$, (d) $X = 0.75$, (e) $X = 1.0$

isothermal sink. When the heat source is in the centre of the enclosure, *Figure 4b* shows that the problem is asymmetric, with two counter-rotating cells. The strengths of circulation are $\Psi_{max} = 16.93$ and 15.4984, which show a slightly more favourable heat transfer to the left. *Figure 4c* shows the case when the heat source is on the right attached to the corner. The strengths of circulation are $\Psi_{max} = 16.07$ and 20.1439, showing more favourable heat transfer to the right. The isotherms show steep gradients on the heat source and on the right, supporting this observation.

The normalized mean Nusselt number at various Rayleigh numbers is calculated for these cases and the results are presented in *Figures 5a–5e*. The size of heat source is from $X = 0.05$ in *Figure 5a* to $X = 1.0$ in *Figure 5e*. The corresponding positions ε are shown in each Figure. It is noticed that the observations and comments made with *Figure 3* apply also here with small differences. Further studies obtained for various other D (not shown here) showed similar results with small quantitative differences. These will be discussed next by taking D as parameter.

The normalized mean Nusselt number as a function of the partition position is calculated for $Ra = 10^6$, and various ε and X. The other parameters are $A = 0.50$, $B = 0.50$, $C = 0.30$ and kept constant. Due to symmetry of the problem, D was varied from 0.5 to 1.0, the latter being the limiting case with the partition attached to the enclosure wall (or without partition). The results are presented in *Figure 6*. As expected, the results show that the normalized mean Nusselt number increases with increasing ε and increasing X. It is observed that the variation of the normalized mean Nusselt number with the partition position, D is not discernible when X not

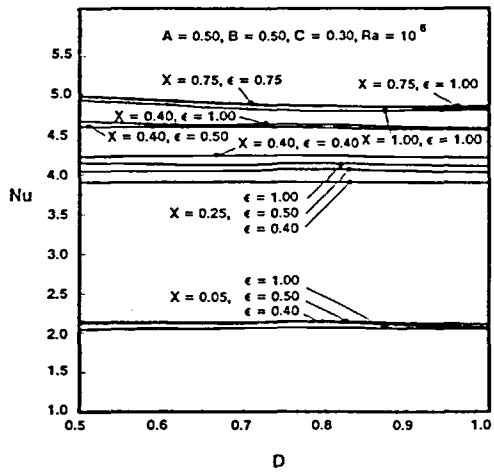

Figure 6 Normalized mean Nusselt number as a function of the partition position D for $Ra = 10^6$ and various X and ε. The other parameters are shown in the Figure

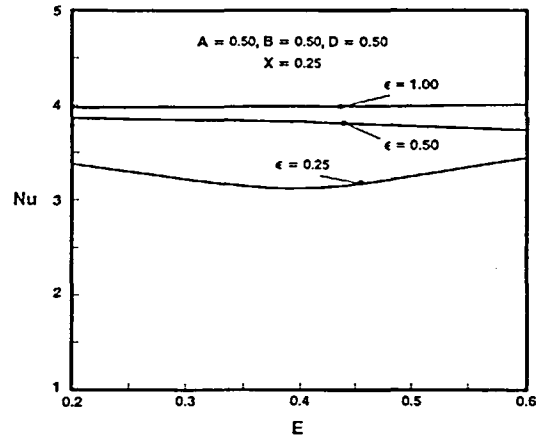

Figure 7 Normalized mean Nusselt number as a function of the partition length E for $Ra = 10^6$ and various ε. The other parameters are shown in the Figure

too large and small variation is present when $X \geqslant 0.75$. This indicates that a short partition of $E = 0.30$ has only little effect on the heat transfer from relatively small heat sources to the isothermal sinks. A slight decrease is observed for the cases of $X = 0.75$ and 1.00 with increasing D. An examination of the streamlines and isotherms for this case showed a slight decrease of convection with increasing D, which has also been verified by using 181 × 21 grid size. For instance, for $X = 1.00$, $\varepsilon = 1.00$, Ψ_{max} was ± 19.94 at $D = 0.50$ and ± 19.35 at $D = 1.00$. This shows that the presence of the partition is to enhance slightly the natural convection.

The effect of the dimensionless partition length is studied for $A = 0.50$, $B = 0.50$, $C = 0.3$, $D = 0.50$, $X = 0.25$ and $Ra = 10^6$ and various ε. The normalized mean Nusselt number as a function of $E = h_1''/H'$ from 0.20 to 0.60 is shown in *Figure 7*. It is seen that the variation of the normalized mean Nusselt number for various ε does not follow a systematic trend. For $\varepsilon = 0.25$, Nu passes from a minimum, for 0.50 it is a decreasing function of E and for 1.00 it is independent of E. It was seen that the mean Nusselt numbers without normalization followed the same trends for three ε values and the heat transfer by conduction was identical for a given ε.

To find out the reason for the observed trends, the streamlines and isotherms are examined. The case with $E = 0.30$ and for the three ε are shown in *Figures 2a* to *2c*. Those for the other two cases at $E = 0.40$ and 0.60 are presented in *Figure 8*. For $\varepsilon = 0.25$ and $E = 0.20$, *Figure 2a* shows a large clockwise circulating cell with a small anti-clockwise circulating cell at the corner. Ψ_{max} and Ψ_{min} are respectively $+15.09$ and -4.88. The heat transfer is by the large clockwise rotating cell effectively to the two sides. For $E = 0.40$ *Figure 8a* shows two cells, a large clockwise circulating cell with decreased strength ($+10.53$) and the other, anti-clockwise circulating with increased strength (-14.11). The heat transfer is mainly by the anti-clockwise cell and in a lesser degree by the clockwise cell. Due to competition between the two, the heat transfer is reduced to the right hand side with respect to $E = 0.30$ case. For $E = 0.60$ *Figure 8d* shows two cells, the clockwise circulating cell with slightly reduced strength ($+9.87$) and the other with further increased strength (-18.90). The heat transfer in this case is enhanced and is mainly by the anti-clockwise cell with additional contribution by the clockwise cell. The isotherms show steep gradients near the left side for $E = 0.30$. The gradients become smaller for $E = 0.40$ and increasing again with increasing E at 0.60.

For $\varepsilon = 0.50$ *Figure 2b* and *Figures 8b* and *8e* show similar phenomena: the strength of

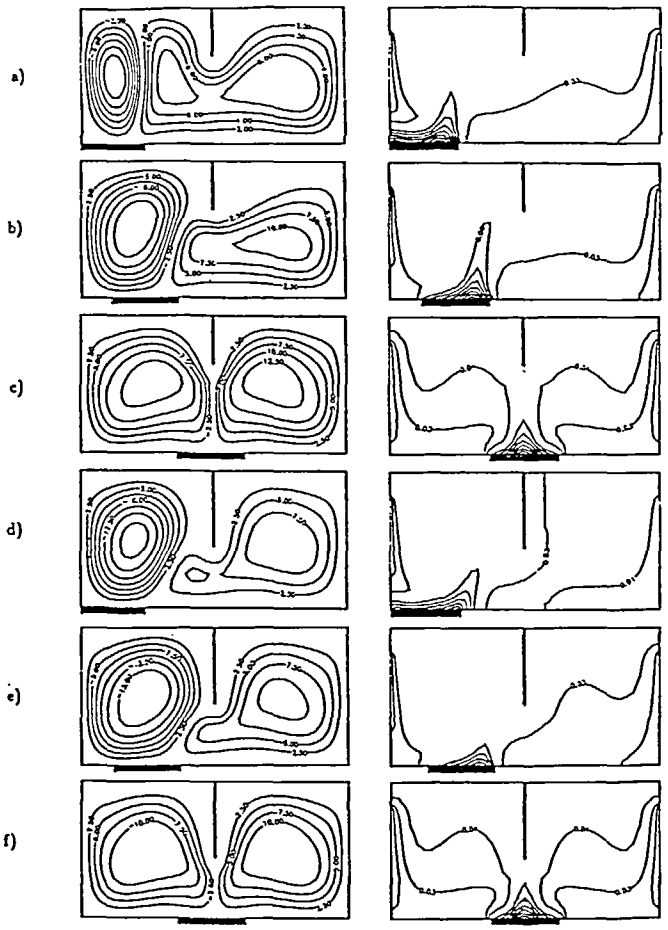

Figure 8 Streamlines (on the left) and isotherms (on the right) for $Ra = 10^6$, $A = 0.5$, $B = 0.5$, $C = 0.3$, $D = 0.5$, $X = 0.25$ and various E. (a) $E = 0.40, \varepsilon = 0.25, \Psi_{min} = -14.11, \Psi_{max} = 10.53$; (b) $E = 0.40$, $\varepsilon = 0.50$, $\Psi_{min} = -17.66$, $\Psi_{max} = 11.30$; (c) $E = 0.40$, $\varepsilon = 1.00$, $\Psi_{min} = -14.16, \Psi_{max} = 14.16$; (d) $E = 0.60, \varepsilon = 0.25, \Psi_{min} = -18.90$, $\Psi_{max} = 9.82$; (e) $E = 0.60, \varepsilon = 0.50, \Psi_{min} = -17.46, \Psi_{max} = 11.07$; (f) $E = 0.60$, $\varepsilon = 1.00$, $\Psi_{min} = -13.08$, $\Psi_{max} = 13.08$

clockwise cell decreases with increasing E (from $+11.75$ to $+10.95$ and then $+10.75$) and that of the anti-clockwise increases slightly with E (from -16.03 to -17.07 and then -17.35). Thus, the heat transfer is decreased with increasing E that can also be seen from the isotherms for this case.

Figure 2c and *Figure 8c* and *8f* show for $\varepsilon = 1.00$ that increasing partition length has the effect of splitting the two cells towards the isothermal heat sinks. But there is not a discernible difference in heat transfer.

The effect of the aspect ratio A on the heat transfer is studied for $B = 0.50$, $C = 0.30$, $D = 0.50$, $E = 0.20$, $X = 0.25$, $Ra = 10^6$ and various ε. The normalized mean Nusselt number as a function of A is shown in *Figure 9*. It should be noted that for a constant L', smaller A corresponds to smaller H' and $X = 0.25$ corresponds to a constant heat source length L'_2. However, ε becomes variable for a given position of heat source since it is normalized with H'. In *Figure 9*, curve

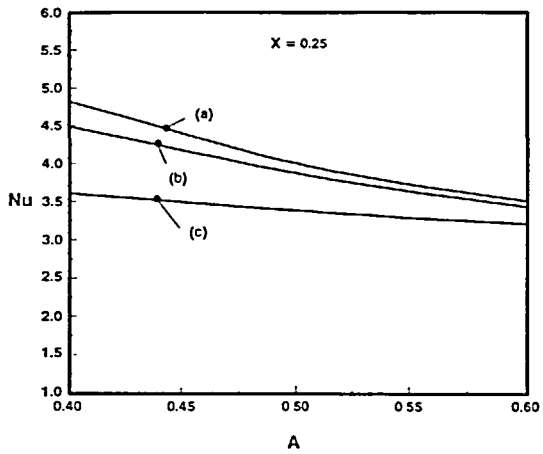

Figure 9 Normalized mean Nusselt number as a function of the aspect ratio A for $Ra = 10^6$ and various heat source positions. The other parameters are shown in the Figure. (a) Heat source is located at the centre of enclosure; (b) heat source is located between centre and the left corner; (c) heat source is attached to the left corner

(a) corresponds to $\varepsilon = 1$ (i.e., the heat source is located at the centre), (b) corresponds to $\varepsilon = 0.5$ and (c) to $\varepsilon = 0.25$ (i.e., heat source is attached to the left corner), all at $A = 0.50$. Further, since Ra is defined with length scale H', for a constant Ra, heat flux is larger for smaller A. *Figure 9* shows that Nu is a decreasing function of A for a given position of heat source and when the heat source is located at more off centre. An examination of the mean Nusselt numbers (non-normalized) showed that they were also decreasing functions of A and heater position for all the cases. This is expected since, for a constant Ra, smaller A corresponds to larger heat flux from a heat source of the same size. Also, heat transfer is larger when the heat source more centrally located in the enclosure. Hence, the heat transfer to the isothermal surfaces becomes enhanced for smaller A with the other parameters being kept the same.

CONCLUSIONS

A numerical study of natural convection heat transfer in two-dimensional partitioned enclosures with localized heating from below has been carried out. The solutions have been obtained by solving the Navier–Stokes and energy equations, using the Boussinesq approximation. The following conclusions are drawn:

(i) heat transfer becomes dominated by natural convection at lower Rayleigh numbers when the length of heat source is bigger and its position is more central in the enclosure;

(ii) position of partition and its length have little effect on heat transfer for a given Rayleigh number. Small effects of partition position are produced when length of heat source is large and its position is central. Also, small effects of partition length are observable when position of heat source is more off centre;

(iii) for a given condition, the heat transfer is enhanced when the enclosure aspect ratio is smaller.

ACKNOWLEDGEMENTS

The financial support by the Natural Sciences and Engineering Research Council of Canada is acknowledged.

REFERENCES

1 Torrance, K. E. and Rockett, J. A. Numerical study of natural convection in an enclosure with localized heating from below—creeping flow to the onset of laminar instability, *J. Fluid Mech.*, **36**, 33–54 (1969)
2 Torrance, K. E., Orloff, L. and Rockett, J. A. Experiments on natural convection in enclosures with localized heating from below, *J. Fluid Mech.*, **36**, 21–31 (1969)
3 Tamotsu, H., Utaro, I. and Teiriki, T. Heat transfer by natural convection in an enclosed cavity—a part of bottom is heated, *Kagaku Kogaku Konbunshu*, **1**, 450–453 (1975) (in Japanese)
4 Chao, P., Ozoe, H., Churchill, S. and Lior, N. Laminar natural convection in an inclined rectangular box with the lower surface half-heated and half-insulated, *J. Heat Transfer*, **105**, 425–432 (1983)
5 Kamotani, Y., Wang, L. W. and Ostrach, S. Natural convection heat transfer in a water layer with localized heating from below, *21st Nat. Heat Transf. Conf., Seattle*, Vol. 26, pp. 43–48 (1983)
6 Hasnaoui, M., Bilgen, E. and Vasseur, P. Multiplicity of solutions and heat transfer by natural convection in a rectangular cavity partially heated from below, *Proc. ASME/JSME Therm. Eng. Joint Conf., Reno, NV*, Vol. 1, pp. 69–75 (1991)
7 Woods, L. C. A note of the numerical solution of fourth differential equations, *Aero Q.*, **5**, 176–184 (1954)
8 Roache, P. *Computational Fluid Dynamics*, Hermosa, Albuquerque (1976)
9 Bassani, J. L., Nansteel, M. W. and November, M. Adiabatic-isothermal boundary conditions in heat transfer, *J. Heat Mass Transfer*, **80**, 903–909 (1987)
10 De Vahl Davis, G. Natural convection of air in a square cavity: a bench mark numerical solution, *Int. J. Num. Meth. Fluids*, **3**, 249–264 (1983)
11 De Vahl Davis, G. and Jones, I. P. Natural convection in a square cavity: a comparison exercise, *Int. J. Num. Meth. Fluids*, **3**, 227–248 (1983)